

Published in final edited form as:

Langmuir. 2011 March 15; 27(6): 2904–2909. doi:10.1021/la2000409.

## Preparation of a Versatile Bifunctional Zeolite for Targeted Imaging Applications

Nicholas Ndiege, Renugan Raidoo, Michael K. Schultz, and Sarah Larsen

Department of Chemistry, University of Iowa, Iowa City, IA 52242

### Abstract

Bifunctional zeolite Y was prepared for use in targeted *in vivo* molecular imaging applications. The strategy involved functionalization of the external surface of zeolite Y with chloropropyltriethoxysilane followed by reaction with sodium azide to form azide-functionalized NaY, which is amenable to copper(I) catalyzed click chemistry. In this study, a model alkyne (4-pentyn-1-ol) was attached to the azide-terminated surface via click chemistry to demonstrate feasibility for attachment of molecular targeting vectors (e.g., peptides, aptamers) to the zeolite surface. The modified particle efficiently incorporates the imaging radioisotope gallium-68 (<sup>68</sup>Ga) into the pores of the azide-functionalized NaY zeolite to form a stable bifunctional molecular targeting vector. The result is a versatile “clickable” zeolite platform that can be tailored for future *in vivo* molecular targeting and imaging modalities.

### Introduction

Porous silicates and aluminosilicates, such as zeolites and mesoporous silica, are high surface area materials that can be functionalized with molecular targeting vectors (e.g., peptides, aptamers) to enable specific high-affinity binding to *in vivo* molecular targets (such as cell surface receptors). In addition, these materials possess unique properties that enable radionuclides and contrast agent metals to be concentrated for applications in magnetic resonance imaging (MRI)<sup>1–8</sup> and positron emission tomography (PET)<sup>9–11</sup>. The development of nanoscale porous materials thus provides promising opportunities for the preparation of multifunctional nanoparticles that can be used for targeted molecular imaging of human disease.<sup>11–13</sup>

High surface area materials have recently emerged as appealing candidates for applications as advanced materials in fields such as biomedical imaging, drug delivery, sensors, catalysis and separations. Zeolites are in this category of materials and are desirable due to their high surface area but also because of their chemical versatility and low toxicity.<sup>14, 15</sup> Functionality can be imparted to zeolites by grafting with various moieties such as amines, thiols, and carboxylate that can allow chemoselective ligation to take place.<sup>16–18</sup> Aluminosilicate zeolites can also be subjected to ion-exchange such that cations can be loaded into the zeolite resulting in sensitivity towards certain chemical or electromagnetic probes.<sup>19</sup>

Cu(I)-catalyzed “click” chemistry is a technique that has recently proven to be a favorable method for chemically anchoring enzymes and proteins onto surfaces of porous materials.<sup>20–25</sup> Cu(I)-catalyzed “click” chemistry is a 1,3-dipolar cycloaddition of organic azides to

#### Supporting Information

Powder XRD patterns and Scanning Electron Microscope images of NaY-Zeolyst and NaY-nano. This material is available free of charge via the Internet at <http://pubs.acs.org>.

alkynes where conjugation of the binding partners occurs via 1,2,3-triazole linkage. Relative to previous ligation techniques, Cu(I)-catalyzed click chemistry has higher yields, favorable thermodynamics and compatibility with many functional group combinations.

Ion exchange of zeolites has traditionally been utilized for catalytic applications (e.g. hydrocarbon cracking). Recently, this feature has been extended further to impart greater analytical function to zeolitic materials whereby the cation exchanged into the zeolite serves as a chemical probe or contrast agent responsive to a specific analytical technique. One example is the exchange of  $Gd^{3+}$  into NaY for use as an MRI (magnetic resonance imaging) agent.<sup>1-3, 6</sup> Recently, Tsotsalas and coworkers demonstrated through *in vivo* studies that  $^{111}In$  could be encapsulated in functionalized zeolite L in which the channels were blocked with a stopcock molecule to prevent leakage of the  $^{111}In$ .<sup>10, 11</sup> The study further showed that the stability of the zeolite L *in vivo* was very high.

In the proof of concept study reported here, the cation exchange of NaY zeolites and Cu(I)-catalyzed “click” chemistry are coupled together to yield a bifunctional zeolite scaffold that can be functionalized with a variety of molecular targeting vectors (e.g., peptides, aptamers), while maintaining cation-absorptive characteristics that enable high efficiency labeling with radionuclides and contrast agent metals for imaging applications. The potential advantages of bifunctional-zeolite-based molecular targeting vectors is two-fold. First, by virtue of their surface area properties, zeolite particles enable addition of multiple targeting vectors per particle. Such multivalency promises to improve the avidity of the targeting vector to the tissue of interest. Secondly, the porous nature of the material enables labeling of the targeting vectors with a significantly higher concentration of contrast-agent metal or radionuclide than traditional molecular imaging agents, which generally employ stoichiometric chelator additions to single targeting vector moieties (ie., a single chelator per peptide).<sup>26</sup> These properties promise higher contrast of malignancies that can provide for earlier detection of tumors, more rapid assessments of response to therapies and more precise targeted delivery of drugs.

Within this context, we present the preparation of a “clickable” zeolite platform for targeted imaging applications as shown schematically in Figure 1. Our goal is to prepare an azide-functionalized zeolite that can readily be further modified with molecular targeting vectors, while preserving the capability for high labeling efficiency with radiometals and contrast agent metals. Generator produced  $^{68}Ga$ , a positron-emitting radionuclide with a half-life of 68 minutes, is used to demonstrate the potential for application in PET imaging.<sup>27</sup> A commercial zeolite, NaY (Zeolyst) and an in-house synthesized nanocrystalline NaY were functionalized to prepare an azide-terminated zeolite surface (NaY-AZPTS) that was then reacted with an acetylene moiety in the presence of Cu(I) as shown schematically in Figure 2. Subsequently, the “clicked” zeolite was loaded with gallium ( $^{68}Ga$ ) by traditional aqueous ion-exchange methods to prepare Ga-exchanged NaY-AZPTS. The ion-exchange capacity of aluminosilicate zeolites, such as zeolite Y, is key to the success of this project and represents a major advantage of zeolites relative to other silicate materials, such as mesoporous silica. The stability of the nanocrystalline Y under physiological conditions (pH=7.4) is another important factor and has been investigated by us previously.<sup>15</sup> Gallium will serve as a representative imaging or contrast agent that could be replaced by indium or gadolinium for other imaging applications. The extent of surface functionalization was varied in order to optimize the preparation of the bifunctional GaY-AZPTS. Importantly, our results indicate that the incorporation of  $^{68}Ga$  can be accomplished at room temperature, which will allow preparation of radiolabeled nanoparticles using molecular targeting vectors that may be susceptible to degradation at high temperatures usually required for  $^{68}Ga$ -chelator coupling reactions.<sup>28, 29</sup>

## Experimental Section

### Functionalization of NaY

NaY from Zeolyst International with Si/Al=1.8, a surface area of 617 m<sup>2</sup>/g and micron-sized particles was used in these studies. NaY-nano with a crystal size of approximately 55 nm, a BET specific surface area of 594 m<sup>2</sup>/g ( $S_{\text{ext}}=109 \text{ m}^2/\text{g}$ ) and a Si/Al=1.6 was synthesized according to a literature procedure.<sup>30</sup> The powder x-ray diffraction patterns and scanning electron microscope (SEM) images for NaY (Zeolyst) and NaY-nano are provided as supplementary information. Approximately 4 g of NaY zeolite was vacuum dried at 200°C for 12 hours. After cooling, 50 ml of toluene was added followed by 0.1 ml of 3-chloropropyltrimethoxysilane (CPTS) and 0.2 ml triethylamine catalyst.<sup>31, 32</sup> This mixture was refluxed at 120°C for 12 hours. The suspension was washed with toluene twice and with an ethanol-water (1:1 vol ratio) mixture twice, followed by rinsing twice each with deionized water and then methanol. The solid was dried at 110°C and then crushed using a mortar and pestle. The amount of CPTS added was varied from 0.00515 g CPTS per gram of zeolite to 2.162 g CPTS per gram zeolite and the samples were labeled sequentially with increasing CPTS concentration as *NaY-CPTS-#* for samples prepared from Zeolyst NaY or *NaY-nano-CPTS* for samples prepared from nanocrystalline NaY.

0.5 grams NaY-CPTS was dehydrated by heating to 200°C under vacuum overnight. 50 ml distilled acetonitrile was added to the dehydrated NaY-CPTS and stirred for 2 hours. Sodium azide (equimolar to CPTS per unit gram of zeolite) was added to the suspension and refluxed at 70°C for 12 hours. The mixture was cooled, centrifuged and then sequentially rinsed with water and methanol (twice each time) and dried at 100°C. The resulting azidopropyltriethoxysilane (AZPTS) functionalized zeolite is labeled *NaY-AZPTS-#* and *NaY-nano-AZPTS-#*.

### Cu(I)-catalyzed “Click” Chemistry

10 ml of tert-butanol and water (1:1 mol ratio) was prepared and added to 0.790 mmol sodium ascorbate (C<sub>6</sub>H<sub>7</sub>NaO<sub>6</sub>) and 0.395 mmol copper sulfate (CuSO<sub>4</sub>). This solution was then added to a mixture of the NaY-AZPTS (0.395 mmol N<sub>3</sub>) and 1.185 mmol 4-pentyn-1-ol and stirred for 12 hours. An additional 1.158 mmol of sodium ascorbate was added to the mixture and incubated for an additional 12 hours. The mixture was centrifuged and rinsed with water twice. The solid was further rinsed with 15 ml of 0.1M N,N diethyldithiocarbamate sodium in methanol and then rinsed with 15 ml methanol and finally rinsed with 15 ml acetone. This N,N diethyldithiocarbamate sodium – methanol – acetone rinse sequence was repeated for a total of 3 times. The solid was then dried at 80°C under 10<sup>-2</sup> torr vacuum for 2 days.

### Ion Exchange of NaY with Naturally Occurring Stable Isotopes of Gallium

A 0.2 mM aqueous solution of Ga(NO<sub>3</sub>)<sub>3</sub> was prepared. 0.1 grams of zeolite was added to 190 mL of the 0.2 mM Ga(NO<sub>3</sub>)<sub>3</sub> solution and stirred for 1 h. The suspension was centrifuged and washed with deionized water. The supernatant and solid samples were analyzed using inductively coupled plasma/optical emission spectroscopy (Varian 720-OES) to determine the gallium concentration. ICP/OES analysis on the supernatant was performed directly while the solid residue was digested in an acid cocktail made by adding 0.005 g of solid to 1.68 ml of 70:30 (HCl:HF), 0.56 ml of concentrated HNO<sub>3(l)</sub>, 8.4 ml of 5% boric acid in 14 ml solution.

Leakage experiments were conducted by suspending 0.02 g of Ga exchanged NaY in 10 ml of 0.17 M NaCl solution for 2 days. The mixture was centrifuged and the supernatant was

collected. The solid residue was washed and dried overnight at 110°C. Both the supernatant and the solid were analyzed by ICP/OES as described above.

### Ion Exchange of NaY with the Radioactive Isotope: $^{68}\text{Ga}$

0.0314 g of NaY and 0.0425 g of NaY-AZPTS were preweighed in plastic vials and suspended in 0.0014 ml of distilled water. Pure  $^{68}\text{Ga}$  for these experiments was obtained using a  $^{68}\text{Ga}$  generator (Model IGG100, Eckert Ziegler GmbH, Berlin, Germany) by methods described previously. Briefly,  $^{68}\text{Ga}$  was eluted from the generator module in 10 mL 0.1 M hydrochloric acid (HCl) directly to a cation exchange resin cartridge (StrataXC, 30 mg, 1 mL capacity column, Phenomenex). The resin effectively retains  $^{68}\text{Ga}$ , while allowing residual  $^{68}\text{Ge}$  parent and interfering metallic impurities to pass. Pure  $^{68}\text{Ga}$  is eluted from the cation exchange resin in 400 mL of 98% acetone/0.05 M HCl. Aliquots of this purified  $^{68}\text{Ga}$  solution were then used for labeling experiments. The radioactivities of the supernatant and the solid were measured using an ionization chamber using the recommended dial setting (416, CRC-25R, Capintec, Ramsey, NJ USA).

For each labeling experiment, 0.0001 ml of  $^{68}\text{Ga}$  solution was added to each of the vials containing the zeolite suspensions at room temperature and then was centrifuged immediately. The supernatant was decanted into another vial and radioactivity measurements were obtained for the wet residue and the decanted supernatant using a scintillation counter. The stock sample of 0.2 ml eluted  $^{68}\text{Ga}$  measured 252 MBq.

### Characterization

Surface areas of the NaY, NaY-CPTS and NaY-AZPTS were measured using the BET method on a Nova 4200 Nitrogen Adsorption Instrument (Quantachrome). Approximately 100 mg of zeolite powder was dried overnight at 120 °C under vacuum. A 7-point BET isotherm was recorded and the specific surface area was calculated for each sample. TGA experiments were conducted on a TA Instruments Q500 TGA. Each sample was heated under nitrogen from room temperature to 1000°C at 5.00 °C/min. The results were analyzed using TA Universal Analysis software. FTIR spectra were obtained using a KBr pellet and a Nicolet Nexus 670 FT-IR (Thermo Electron Company) instrument.

## Results and Discussion

### Functionalization of NaY with CPTS and AZPTS

NaY-Zeolyst and NaY-nano were functionalized with CPTS followed by reaction with sodium azide as outlined in Figure 2 with the goal of preparing the zeolite for copper-catalyzed “click chemistry” with a model alkyne. The SEM images and powder XRD patterns for NaY-Zeolyst and NaY-nano are provided as supplementary information (Figures S1 and S2) and indicate crystalline NaY with crystal sizes of ~1  $\mu\text{m}$  and ~55 nm, respectively. In these studies, a model alkyne (4-pentyn-1-ol) was used. Since the objective is to ultimately use a PET radioisotope with a relatively short half-life, the gallium ion-exchange was done after surface functionalization. Initial radioisotope loading experiments were conducted with naturally occurring gallium isotopes ( $^{69}\text{Ga}$  (60.1%) and  $^{71}\text{Ga}$  (39.1%)) which are not radioactive followed by experiments with the radioactive form of  $^{68}\text{Ga}$ .

The extent of functionalization with CPTS on NaY-Zeolyst was varied and the resulting samples were characterized by TGA to measure functional group loading. This data is summarized in Table 1. The CPTS loading was systematically varied from 0 to 0.600 mmol CPTS/g NaY-Zeolyst as reflected in the TGA data in Table 1. Similarly, the subsequent loading with AZPTS after reaction with sodium azide resulted in a range of 0 to 0.486 mmol

AZPTS/g NaY-Zeolyst. A sample of NaY-nano was also functionalized with CPTS followed by AZPTS and the loading levels are listed in Table 1.

The relationship between CPTS loading followed by AZPTS loading is shown in Figure 3 where a roughly one to one correspondence between CPTS and AZPTS loading is observed. Through linear regression, the  $R=0.94$  indicates a strong linear correlation and suggests that the CPTS is quantitatively converted to AZPTS in the second step of the functionalization scheme (Figure 2). As can be seen from the nitrogen adsorption data, the surface area of NaY-AZPTS decreases by approximately 30–70% after functionalization due to the restricted access to the internal pore surface caused by the functional groups on the external surface. This is expected and has been observed previously for functionalized zeolites.<sup>10, 16, 17</sup>

### Click Chemistry with AZPTS Functionalized NaY

The functionalization with CPTS and AZPTS was also monitored by FTIR spectroscopy as shown in Figure 4. The FTIR spectrum of the parent NaY zeolite is shown in Figure 4a. After functionalization with CPTS (Figure 4b), peaks are observed at  $\sim 2900\text{ cm}^{-1}$  in the C-H stretching region of the FTIR spectrum that are attributed to the propyl group of the CPTS. After reaction with AZPTS, a peak assigned to the azide ( $\text{N}_3$ ) is observed at  $\sim 2150\text{ cm}^{-1}$  in the FTIR spectrum (Figure 4c). This peak is assigned as the  $\nu_{\text{as}}(\text{N}_3)$ , the asymmetric azide stretch.<sup>33</sup> After reaction with a model alkyne, 4-pentyn-1-ol, the alkyne is “clicked” and the azide peak at  $\sim 2150\text{ cm}^{-1}$  is no longer observed in the FTIR spectrum (Figure 4d) consistent with the reaction of the azide depicted in Figure 2. To ensure that copper from the copper catalyzed click reaction is not taken up by the NaY zeolite, ICP/OES analysis of the solid sample after the click reaction was conducted and no copper was detected in the solids. If future problems arise due to the use of copper, a copper-free approach to click chemistry will be investigated.<sup>26, 34</sup>

### Gallium uptake on NaY-AZPTS and NaY-clicked

The AZPTS functionalized NaY samples were loaded with gallium via ion-exchange with aqueous naturally occurring  $\text{Ga}(\text{NO}_3)_3$ . Initial experiments were conducted with the gallium stable isotopes followed by experiments with the positron-emitting radionuclide (gallium-68,  $^{68}\text{Ga}$ ), which has a half-life of 68 minutes. Initial experiments indicated that unfunctionalized NaY-Zeolyst had a capacity of 0.9 mmol Ga/g NaY. Functionalized NaY-AZPTS had substantially reduced ion-exchange capacities ranging from approximately 0.1 to 0.2 mmol Ga/g zeolite. The mean gallium loading for the NaY-AZPTS (Zeolyst) samples was 0.16 mmol/g with a standard deviation of 0.04. The gallium uptake did not vary systematically with the extent of functionalization so there is no apparent advantage to limiting the extent of functionalization in order to increase the gallium loading capacity. Therefore, the optimal surface functionalization loading level can be chosen with respect to targeting and biocompatibility considerations.

The gallium loading of the NaY-nano-AZPTS and NaY-nano-clicked were 0.389 and 0.601 mmol/g, respectively, which are higher than the gallium loadings for the Zeolyst NaY samples as indicated in Table 1.

Leakage experiments to test for gallium leakage out of the zeolite were conducted on the unfunctionalized NaY as well as CPTS and AZPTS functionalized Ga-exchanged NaY (Zeolyst). After a period of two days in an aqueous NaCl solution, no leakage of gallium was observed in any of these samples as analyzed by ICP/OES measurements of gallium in the supernatant solution.



Experiments were also conducted with the positron-emitting radioisotope,  $^{68}\text{Ga}$ . The NaY-AZPTS and the parent NaY were ion-exchanged separately with aqueous  $^{68}\text{Ga}$  at room temperature. Each sample was centrifuged immediately and the supernatant was removed from the centrifuge tube. For NaY-AZPTS, radioactivity of the supernatant was found to be 3.7 MBq after exposure to NaY-AZPTS and the radioactivity of the solid was 62 MBq. For the parent NaY, the radioactivity of the supernatant was 1.8 MBq after exposure to NaY and the radioactivity of the solid was 59.8 MBq. These results indicate that the radioactive  $^{68}\text{Ga}$  is taken up by both the parent zeolite and the functionalized NaY-AZPTS in similar amounts. Furthermore, these results demonstrate that the  $^{68}\text{Ga}$  uptake occurs rapidly which is essential when using a radioisotope with a short half-life.

## Conclusions

In this study, a bifunctional zeolite for targeted imaging applications was prepared. NaY zeolite was functionalized with CPTS followed by reaction with sodium azide resulting in an AZPTS functionalized zeolite surface. A model alkyne (4-pentyn-1-ol) was used to demonstrate the feasibility of attaching molecular targeting vectors such as peptides and aptamers to the azide-terminated external surface of the zeolite via copper(I) catalyzed click chemistry. The NaY-AZPTS was loaded with  $^{68}\text{Ga}$ , a positron emitter used in PET imaging. The azide functionalized NaY exhibited remarkably high affinity for  $^{68}\text{Ga}$  at room temperature under aqueous conditions. Thus, the azide terminated zeolite Y has potential to be developed as a versatile platform for targeting imaging applications in which a radioisotope such as  $^{68}\text{Ga}$  or  $^{111}\text{In}$  or a contrast agent, such as Gd, can be incorporated into the interior pore surface of the functionalized zeolite that has been prepared with a targeting functionality on the external surface.

## Supplementary Material

Refer to Web version on PubMed Central for supplementary material.

## Acknowledgments

ND acknowledges support from Grant Number UL1RR024979 from the National Center for Research Resources (NCRR), a part of the National Institutes of Health (NIH). Its contents are solely the responsibility of the authors and do not necessarily represent the official views of the CTSA or NIH. RR acknowledges financial support from Iowa Biosciences Advantage National Institutes of Health (NIGMS 58939). Anton Petushkov is acknowledged for synthesis and characterization of the nanocrystalline NaY sample.

## References

1. Bresinska I, Balkus KJ. Studies of Gd(III)-Exchanged Y-Type Zeolites Relevant to Magnetic-Resonance-Imaging. *J Phys Chem.* 1994; 98(49):12989–12994.
2. Young SW, Qing F, Rubin D, Balkus KJ, Engel JS, Lang J, Dow WC, Mutch JD, Miller RA. Gadolinium Zeolite as an Oral Contrast Agent for Magnetic-Resonance-Imaging. *J Magn Reson Imaging.* 1995; 5(5):499–508. [PubMed: 8574032]
3. Balkus KJ, Shi JM. A study of suspending agents for gadolinium(III)-exchanged hectorite. An oral magnetic resonance imaging contrast agent. *Langmuir.* 1996; 12(26):6277–6281.
4. Lin YS, Hung Y, Su JK, Lee R, Chang C, Lin ML, Mou CY. Gadolinium(III)-incorporated nanosized mesoporous silica as potential magnetic resonance imaging contrast agents. *J Phys Chem B.* 2004; 108(40):15608–15611.
5. Li WS, Li ZF, Jing FY, Yang XG, Li XJ, Pei FK, Wang XX, Lei H. Zeolites  $\text{Mn}^{2+}$ -NaY as oral gastrointestinal tract contrast agents in magnetic resonance imaging. *Acta Chimica Sinica.* 2007; 65(18):2029–2033.

6. Csajbok E, Banyai I, Vander Elst L, Muller RN, Zhou WZ, Peters JA. Gadolinium(III)-loaded nanoparticulate zeolites as potential high-field MRI contrast agents: Relationship between structure and relaxivity. *Chem-Eur J*. 2005; 11(16):4799–4807. [PubMed: 15929138]
7. Taylor KML, Kim JS, Rieter WJ, An H, Lin WL, Lin WB. Mesoporous silica nanospheres as highly efficient MRI contrast agents. *J Am Chem Soc*. 2008; 130(7):2154. [PubMed: 18217764]
8. Taylor KML, Rieter WJ, Lin WB. Manganese-Based Nanoscale Metal–Organic Frameworks for Magnetic Resonance Imaging. *J Am Chem Soc*. 2008; 130(44):14358. [PubMed: 18844356]
9. Matheoud R, Secco C, Ridone S, Inglese E, Brambilla M. The use of molecular sieves to simulate hot lesions in F-18-fluorodeoxyglucose - positron emission tomography imaging. *Phys Med Biol*. 2008; 53(8):N137–N148. [PubMed: 18379022]
10. Tsotsalas MM, Kopka K, Luppi G, Wagner S, Law MP, Schafers M, De Cola L. Encapsulating In-111 in Nanocontainers for Scintigraphic Imaging: Synthesis, Characterization, and In Vivo Biodistribution. *ACS Nano*. 2010; 4(1):342–348. [PubMed: 20020752]
11. Tsotsalas M, Busby M, Gianolio E, Aime S, De Cola L. Functionalized nanocontainers as dual magnetic and optical probes for molecular imaging applications. *Chem Mater*. 2008; 20(18):5888–5893.
12. Kim J, Kim HS, Lee N, Kim T, Kim H, Yu T, Song IC, Moon WK, Hyeon T. Multifunctional Uniform Nanoparticles Composed of a Magnetite Nanocrystal Core and a Mesoporous Silica Shell for Magnetic Resonance and Fluorescence Imaging and for Drug Delivery. *Angew Chem Int Edit*. 2008; 47(44):8438–8441.
13. Liong M, Lu J, Kovoichich M, Xia T, Ruehm SG, Nel AE, Tamanoi F, Zink JI. Multifunctional inorganic nanoparticles for imaging, targeting, and drug delivery. *ACS Nano*. 2008; 2(5):889–896. [PubMed: 19206485]
14. Petushkov A, Intra J, Graham JB, Larsen SC, Salem AK. Effect of Crystal Size and Surface Functionalization on the Cytotoxicity of Silicalite-1 Nanoparticles. *Chem Res Toxicol*. 2009; 22(7):1359–1368. [PubMed: 19580308]
15. Petushkov A, Freeman J, Larsen SC. Framework Stability of Nanocrystalline NaY in Aqueous Solution at Varying pH. *Langmuir*. 2010; 26(9):6695–6701. [PubMed: 20099832]
16. Song W, Woodworth JF, Grassian VH, Larsen SC. Microscopic and macroscopic characterization of organosilane-functionalized nanocrystalline NaZSM-5. *Langmuir*. 2005; 21(15):7009–7014. [PubMed: 16008416]
17. Zhan BZ, White MA, Lumsden M. Bonding of organic amino, vinyl, and acryl groups to nanometer-sized NaX zeolite crystal surfaces. *Langmuir*. 2003; 19:4205–4210.
18. Cheng CH, Bae TH, McCool BA, Chance RR, Nair S, Jones CW. Functionalization of the internal surface of pure-silica MFI zeolite with aliphatic alcohols. *J Phys Chem C*. 2008; 112(10):3543–3551.
19. Breck, DW. *Zeolite Molecular Sieves: Structure, Chemistry, and Use*. Wiley-Interscience; New York: 1974. p. 752
20. Chassaing S, Kumarraja M, Sido ASS, Pale P, Sommer J. Click chemistry in Cu-I-zeolites: The Huisgen 3+2 -cycloaddition. *Org Lett*. 2007; 9(5):883–886. [PubMed: 17286410]
21. Kolb HC, Finn MG, Sharpless KB. Click chemistry: Diverse chemical function from a few good reactions. *Angew Chem Int Edit*. 2001; 40(11):2004.
22. Moses JE, Moorhouse AD. The growing applications of click chemistry. *Chem Soc Rev*. 2007; 36:1249–1262. [PubMed: 17619685]
23. Chassaing S, Sido ASS, Alix A, Kumarraja M, Pale P, Sommer J. “Click Chemistry” in zeolites: Copper(I) zeolites as new heterogeneous and ligand-free catalysts for the Huisgen [3+2] cycloaddition. *Chem-Eur J*. 2008; 14(22):6713–6721. [PubMed: 18576412]
24. Schlossbauer A, Schaffert D, Kecht J, Wagner E, Bein T. Click chemistry for high-density biofunctionalization of mesoporous silica. *J Am Chem Soc*. 2008; 130(38):12558. [PubMed: 18759397]
25. Huang L, Dolai S, Raja K, Kruk M. “Click” Grafting of High Loading of Polymers and Monosaccharides on Surface of Ordered Mesoporous Silica. *Langmuir*. 2010; 26(4):2688–2693. [PubMed: 20141209]

26. Martin ME, Parameswarappa SG, O'Dorisio MS, Pigge FC, Schultz MK. A DOTA-peptide conjugate by copper-free click chemistry. *Bioorg Med Chem Lett*. 2010; 20(16):4805–4807. [PubMed: 20630750]
27. Fani M, Andre JP, Maecke HR.  $^{68}\text{Ga}$ -PET: a powerful generator-based alternative to cyclotron-based PET radiopharmaceuticals. *Contrast Media & Molecular Imaging*. 2008; 3:53–63. [PubMed: 18383455]
28. Zhernosekov KP, Filosofov DV, Baum RP, Aschoff P, Bihl H, Razbash AA, Jahn M, Jennewein M, Rosch F. Processing of generator-produced Ga-68 for medical application. *J Nucl Med*. 2007; 48(10):1741–1748. [PubMed: 17873136]
29. Virgolini I, Ambrosini V, Bomanji JB, Baum RP, Fanti S, Gabriel M, Papathanasiou ND, Pepe G, Oyen W, De Cristoforo C, Chiti A. Procedure guidelines for PET/CT tumour imaging with Ga-68-DOTA-conjugated peptides: Ga-68-DOTA-TOC, Ga-68-DOTA-NOC, Ga-68-DOTA-TATE. *Eur J Nucl Med Mol Imaging*. 2010; 37(10):2004–2010. [PubMed: 20596866]
30. Song W, Grassian VH, Larsen SC. High yield method for nanocrystalline zeolite synthesis. *Chem Commun*. 2005; (23):2951–2953.
31. Adam F, Osman H, Hello KM. The immobilization of 3-(chloropropyl)triethoxysilane onto silica by a simple one-pot synthesis. *J Colloid Interface Sci*. 2009; 331(1):143–147. [PubMed: 19095242]
32. Nunes CD, Valente AA, Pillinger M, Fernandes AC, Romao CC, Rocha J, Goncalves IS. MCM-41 functionalized with bipyridyl groups and its use as a support for oxomolybdenum(VI) catalysts. *J Mater Chem*. 2002; 12(6):1735–1742.
33. Malvi B, Sarkar BR, Pati D, Mathew R, Ajithkumar TG, Sen Gupta S. “Clickable” SBA-15 mesoporous materials: synthesis, characterization and their reaction with alkynes. *J Mater Chem*. 2009; 19(10):1409–1416.
34. Schultz MK, Parameswarappa SG, Pigge FC. Synthesis of a DOTA-Biotin Conjugate for Radionuclide Chelation via Cu-Free Click Chemistry. *Org Lett*. 2010; 12(10):2398–2401. [PubMed: 20423109]



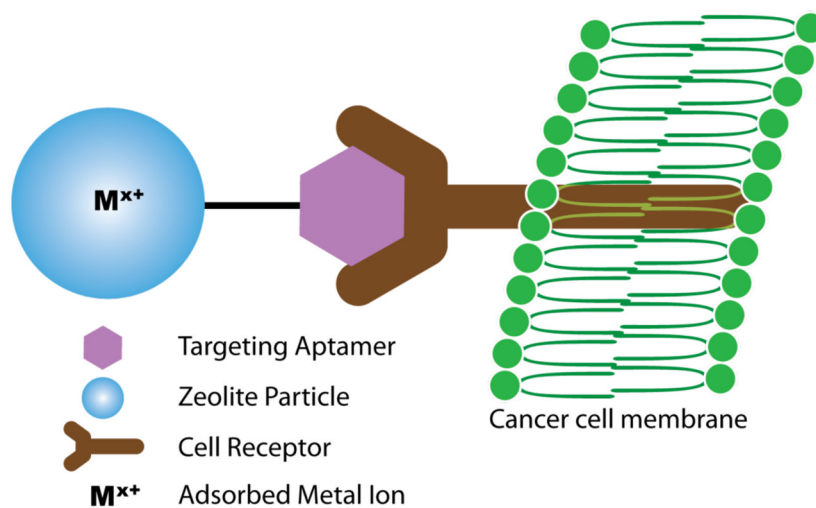


**Figure 1.** Overall strategy for use of the bifunctional zeolite in targeted imaging applications.

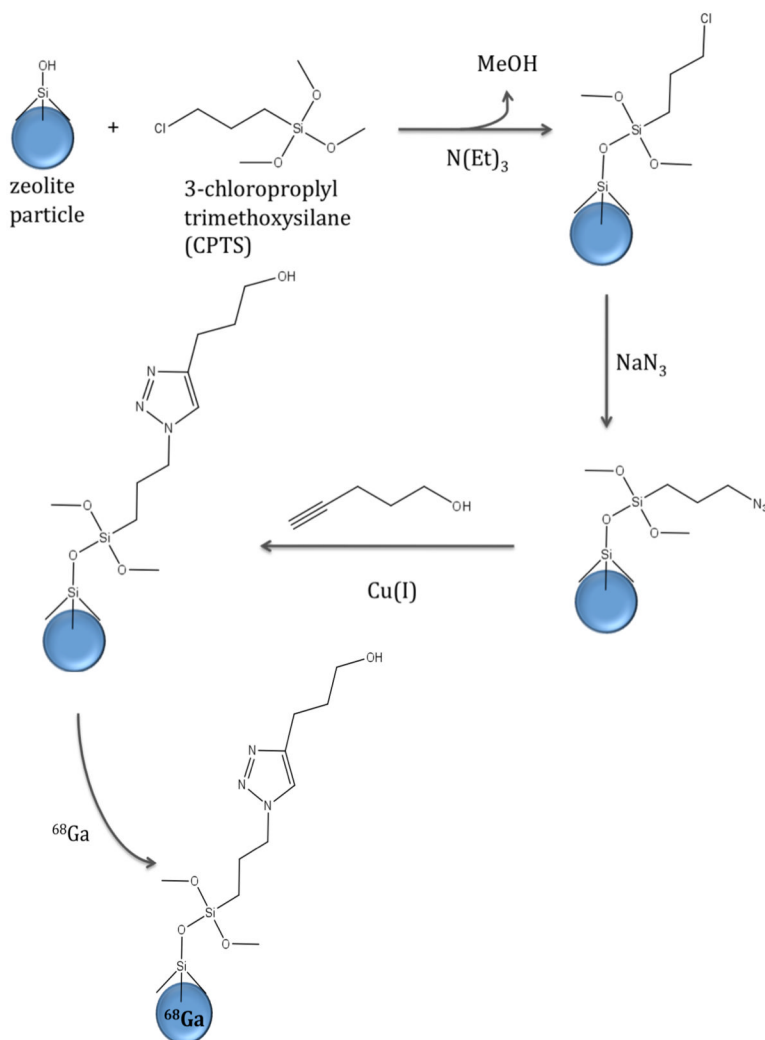


**Figure 2.** Reaction scheme for functionalization of zeolite NaY with CPTS and AZPTS followed by click chemistry with a model alkyne.

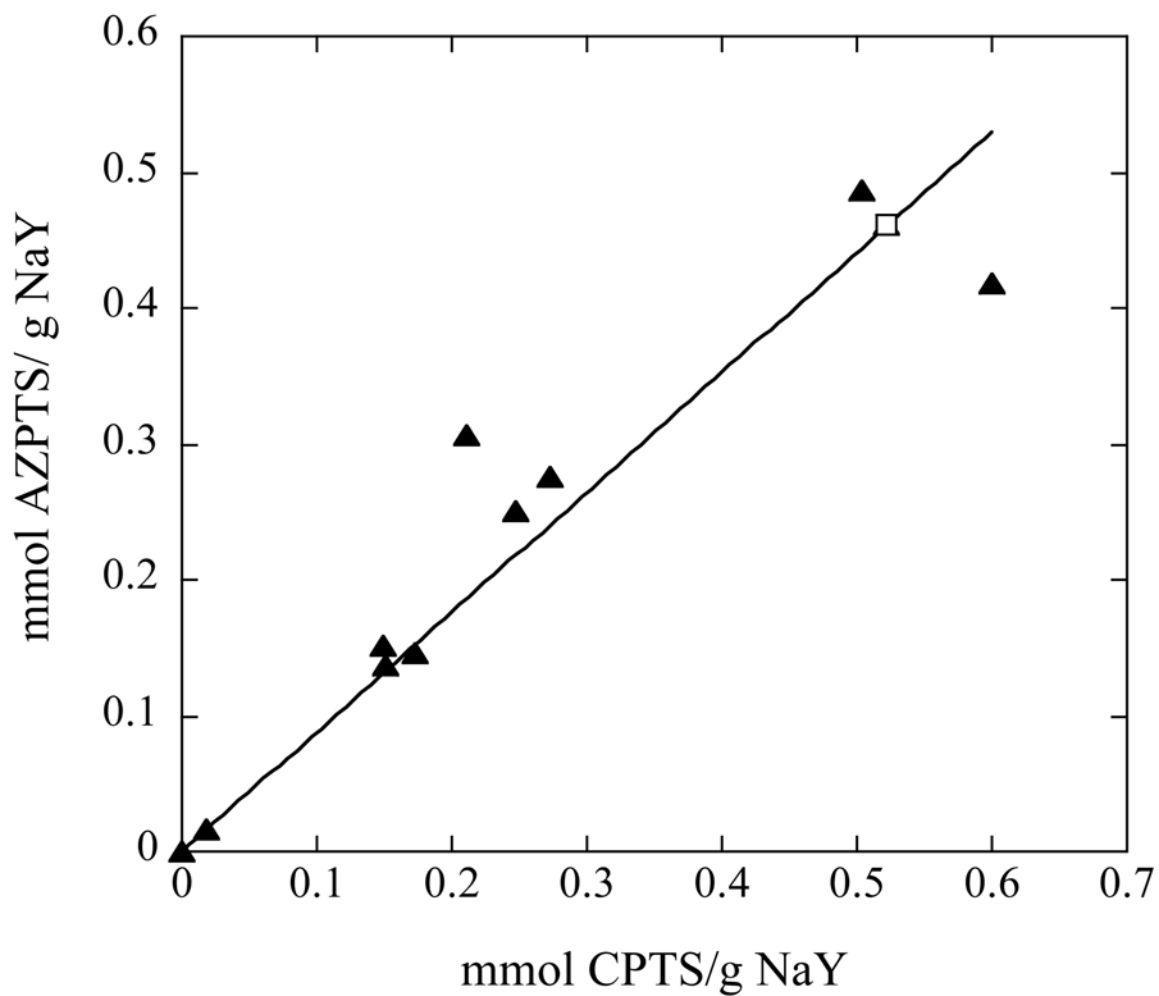


**Figure 3.** The CPTS loading (measured by TGA) is plotted versus the subsequent AZPTS loading (measured by TGA). The filled triangles represent data from NaY-Zeolyst samples and the open square represents NaY-nano.

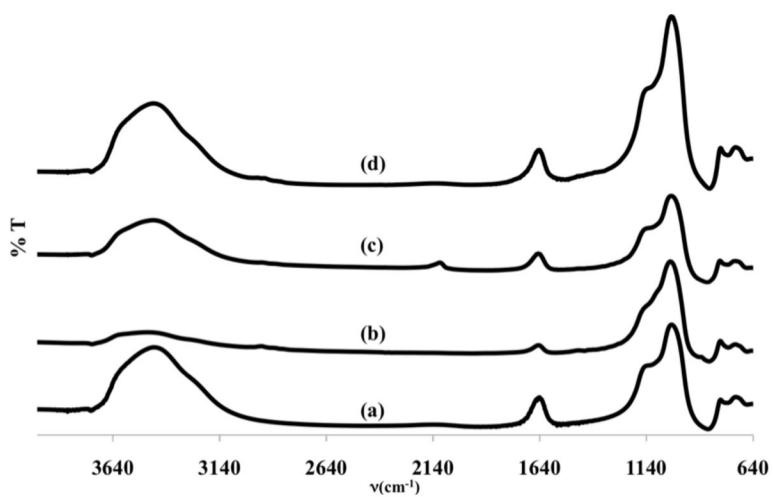


**Figure 4.** FTIR spectra of a) NaY, b) NaY-CPTS-8(0.504 mmol/g loading), c) NaY-AZPTS-8 (0.486 mmol/g loading) and d) NaY-AZPTS-8 clicked with 4-propynol.

**Table 1**Surface area, functional group loading and Ga<sup>3+</sup> uptake functionalized NaY.

Sample	Surface Area <sup>a</sup> , m <sup>2</sup> /g	CPTS loading <sup>b</sup> mmol/g zeolite	AZPTS loading <sup>b</sup> mmol/g zeolite	Ga uptake <sup>c</sup> mmol/g zeolite
NaY(Zeolyst)	617	NA	NA	0.907
NaY-AZPTS-1	325	0.018	0.017	0.179
NaY-AZPTS-2	270	0.149	0.152	0.162
NaY-AZPTS-3	377	0.151	0.138	0.108
NaY-AZPTS-4	402	0.173	0.147	0.134
NaY-AZPTS-5	289	0.211	0.306	0.185
NaY-AZPTS-6	293	0.247	0.250	0.205
NaY-AZPTS-7	358	0.273	0.275	0.185
NaY-AZPTS-8	414	0.504	0.486	0.098
NaY-AZPTS-9	187	0.600	0.418	0.120
NaY-nano	594	NA	NA	0.398
NaY-nano-AZPTS	255	0.522	0.461	0.389
NaY-nano-AZPTS-clicked	255	0.522	0.461	0.601

<sup>a</sup> Surface area was measured by the BET method. The estimated error is  $\pm 5$  m<sup>2</sup>/g.

<sup>b</sup> Functional group loading was measured by TGA.

<sup>c</sup> Gallium uptake was measured by ICP/OES analysis of the supernatants.